

## General Disclaimer

### One or more of the Following Statements may affect this Document

- This document has been reproduced from the best copy furnished by the organizational source. It is being released in the interest of making available as much information as possible.
- This document may contain data, which exceeds the sheet parameters. It was furnished in this condition by the organizational source and is the best copy available.
- This document may contain tone-on-tone or color graphs, charts and/or pictures, which have been reproduced in black and white.
- This document is paginated as submitted by the original source.
- Portions of this document are not fully legible due to the historical nature of some of the material. However, it is the best reproduction available from the original submission.

**NASA TECHNICAL  
MEMORANDUM**

NASA TM X-62,454

NASA TM X-62,454

(NASA-TM-X-62454) ON THE FEASIBILITY OF  
REAL-TIME PREDICTION OF AIRCRAFT CARRIER  
MOTION AT SEA (NASA) 25 p HC \$3.50 CSCL 13J

N76-15834

G3/65    Unclas  
         08545

**ON THE FEASIBILITY OF REAL-TIME PREDICTION OF  
AIRCRAFT CARRIER MOTION AT SEA**

Menahem Sidar and Brian F. Doolin

Ames Research Center  
Moffett Field, Calif. 94035



June 1975

1. Report No. NASA TM X-62,454	2. Government Accession No.	3. Recipient's Catalog No.	
4. Title and Subtitle ON THE FEASIBILITY OF REAL-TIME PREDICTION OF AIRCRAFT CARRIER MOTION AT SEA		5. Report Date	
		6. Performing Organization Code	
7. Author(s) Menahem Sidar <sup>1</sup> and Brian F. Doolin		8. Performing Organization Report No. A-6169	
9. Performing Organization Name and Address Ames Research Center Moffett Field, California 94035		10. Work Unit No. 505-07-11	
		11. Contract or Grant No.	
12. Sponsoring Agency Name and Address National Aeronautics and Space Administration Washington, D.C. 20546		13. Type of Report and Period Covered Technical Memorandum	
		14. Sponsoring Agency Code	
15. Supplementary Notes  <sup>1</sup> NRC Research Associate			
16. Abstract  Landing aircraft on board carriers is a most delicate phase of flight operations at sea. The ability to predict the aircraft carrier's motion over an interval of several seconds within reasonable error bounds may allow an improvement in touchdown dispersion and a more certain value for ramp clearance due to a smoother aircraft trajectory. Also, improved information to the Landing Signal Officer should decrease the number of waveoffs substantially.  This paper indicates and shows quantitatively that, based on the power density spectrum data for pitch and heave measured for various ships and sea conditions, the motion can be predicted well for up to 15 seconds. Moreover, the zero crossover times for both pitch and heave motions can be predicted with impressive accuracy.  The predictor was designed on the basis of Kalman's optimum filtering theory for the discrete time case, adapted for real-time digital computer operation.			
17. Key Words (Suggested by Author(s))  Kalman filtering Ship motion prediction Real time prediction		18. Distribution Statement  Unlimited  STAR Category - 65	
19. Security Classif. (of this report) Unclassified	20. Security Classif. (of this page) Unclassified	21. No. of Pages 24	22. Price* \$ 3.25

On the Feasibility of Real-Time  
Prediction of Aircraft Carrier Motion at Sea

MENACHEM SIDAR<sup>1</sup>

BRIAN F. DOOLIN

Ames Research Center, NASA

Moffett Field, Calif. 94035

Abstract

Landing aircraft on board carriers is a most delicate phase of flight operations at sea. The ability to predict the aircraft carrier's motion over an interval of several seconds within reasonable error bounds may allow an improvement in touchdown dispersion and a more certain value for ramp clearance due to a smoother aircraft trajectory. Also, improved information to the Landing Signal Officer should decrease the number of waveoffs substantially.

This paper indicates and shows quantitatively that, based on the power density spectrum data for pitch and heave measured for various ships and sea conditions, the motion can be predicted well for up to 15 seconds. Moreover, the zero crossover times for both pitch and heave motions can be predicted with impressive accuracy.

The predictor was designed on the basis of Kalman's optimum filtering theory for the discrete time case, adapted for real-time digital computer operation.

<sup>1</sup>NRC Research Associate

## I. Introduction

The landing phase of an aircraft aboard an aircraft carrier represents a complex operation and a demanding task. The last 10 to 15 seconds before aircraft touchdown involves terminal guidance and control problems, where not only the aircraft is disturbed by several kinds of stochastic (wind) disturbances, but also the touchdown point (on the ship) is being moved randomly. Despite the wind disturbances and the final point (target) random motion, the landing accuracy specified for carrier operations is very high, i.e., a few tens of feet longitudinal landing dispersion. Such a terminal point problem is made tractable in a most natural way by assuming that the ship's position can be predicted for several seconds ahead so that the airplane is guided toward the future position of the touchdown point. The scope of this study was to establish to what extent a stochastic process, like the ship's motion, is predictable over moderate periods of time.

Quantitative results obtained throughout this predictor's feasibility study concerning the relationship between the prediction error versus the prediction time, the influence of measurement noise, and the "narrowness" effect of the ship motion power density spectrum are presented. Digital simulations show that the prediction accuracy does not degrade prohibitively even for quite large measurement noise.

A variety of possibilities with respect to the incorporation of the prediction algorithm in the Aircraft Carrier Landing System (ACLS)

can be investigated, but those topics are out of the scope of this paper. Their common denominator consists of the ability to predict the ship's motion in heave and pitch for periods of 12 to 15 seconds. Feasibility of predicting the ship's motion within acceptable bounds of error can also lead to improvement of the Landing Signal Officer (LSO) decision policy for waveoffs.

The need for prediction for carrier landing operations was pointed out several years ago by Durand [1], Durand and Wasicko [2], Kaplan [3], and Siewert and A'Harrah [4]. Loeb [5] also indicated the need for predicting the ship's motion.

A tremendous amount of theoretical modeling, experimental results, and the collection of a large amount of data over the years are discussed by Powell and Theoclitus [6], Kaplan [3], Johnson [7], and many others.

A study of prediction techniques for aircraft carrier motions at sea was done by Kaplan [3], who considered a deterministic technique based on a convolution integral representation with wave height measurements at the bow serving as input. He derived, from the ship response time-history functions, a Kernel-type weighting function which operated on the measurements in order to provide the predicted motion history. Model test data indicated that this technique yielded ship's pitch prediction for up to 6 seconds, but the method suffers from severe limitations and practical implementation difficulties. A hybrid prediction technique, based on modern control theory, was suggested in [5] as a possible future approach.

Our approach was to make a rather direct use of the ship's motion characteristics and the measuring instrumentation existing on board the ship in order to get the predicted motion. Using this information, a predictor based on Kalman's theory of optimum estimation was designed.

Several circumstances contribute to the success of this approach. The size and mass of the ship significantly filter the motion of the sea. A complete landing operation is short enough that the stochastic processes are reasonably taken to be stationary. Finally, the prediction interval is only a small fraction of the time it takes each aircraft to land.

This paper is divided into three parts: 1) the derivation of the mathematical model of the ship's motion, 2) the rationale for the predictor implementation, including the Kalman filter and predictor equations, and 3) discussion of some of the results obtained. Since we are interested only in the most critical aspects of the landing operation, namely the characteristics of the longitudinal channel, we merely investigate in the sequel the predictability of the pitch and heave motion of the ship.

## II. Modeling the Carrier Motion

As we pointed out before, quite a large amount of data exists describing the motion of aircraft carriers at sea. Extensive experiments and simulations have been carried out, both at sea and in water tanks, establishing frequency response curves and power spectral density functions (psdf) as a means of representing ship pitch and heave motion characteristics for utilization in a systems analysis of the whole carrier-aircraft landing system.

Power spectral density functions describing, globally, the statistical behavior of the pitch and the heave motions have been established and measured for several types of carriers at different sea conditions [6],[7]. An analysis and a close comparison of these data reveal that the psdf,  $\phi(\omega)$ , where  $\omega$  is the carrier motion frequency in radians per second, is not affected too sensibly either by the type of the carrier or by the sea conditions (see [7]). Moreover, the function peaks sharply around a center frequency of about

Fig 1  $\omega_0 = 0.60 \text{ rad sec}^{-1}$  (Fig. 1), the sea state changing the value of the peak at  $\omega = \omega_0$  (see [7]).

Fig 2 Data obtained from basin model experimentation confirm (Fig. 2) the measured power density spectrum, showing the same narrow-band aspect, but centered at  $\omega_0 \approx 0.75 \text{ rad sec}^{-1}$ .

It is obvious, also, that for the prediction periods of interest, we can make the plausible assumption that the ship heave motion  $\underline{z}(t)$  and pitch motion  $\theta(t)$  are stationary, narrow-band, stochastic processes. Both processes are actually continuously measured aboard the ship as a part of the SPN-42 ACLS, the measurements being contaminated by random noises  $\underline{v}(t)$  and  $\underline{w}(t)$ , respectively (see [8]).

In order to obtain the mathematical model of  $\phi_{\underline{z}}(\omega)$  and  $\phi_{\theta}(\omega)$  for the ship's heave and pitch, we take the innovation process point of view; namely, we assume that  $z(t)$  and  $\theta(t)$  are stochastic processes generated by a white, Gaussian, random process passing through a causal and invertible lumped transfer function  $\underline{G}_{\underline{z}}(\underline{s})$  or  $\underline{G}_{\theta}(\underline{s})$  (see [9]).

The first step of the procedure is to approximate the experimentally obtained density functions  $\phi_{\underline{z}}(\omega)$  and  $\phi_{\theta}(\omega)$  by analytic



expressions that accurately represent the important part of the spectrum.

As a result, one obtains a single, equivalent transfer function

$\underline{G}_z(s) = G_\theta(s) = \underline{G}_s(s)$  of the filter acting on the Gaussian noise, which is essentially the same for both the pitch and heave motions and is given in (1):

$$\underline{G}_s(s) = \underline{g}s / (s^2 + \underline{a}s + \underline{d}) \quad (1)$$

with the following nominal values for  $\underline{g}$ ,  $\underline{a}$ , and  $\underline{d}$ :  $\underline{g} = 0.6$ ,  $\underline{a} = 0.06$ ,  $\underline{d} = 0.36$ . This approximation is "pessimistic" with respect to the prediction problem, as is shown by the comparison with  $\phi(\omega)$  in Fig. 1.

The reason for this pessimistic approach is twofold: 1) to avoid running into high-dimensional systems unnecessarily, and 2) to obtain conservative values for the maximum achievable prediction time.

From (1), by making use of the usual "half power" definition of the bandwidth for a narrow-band process, equivalent bandwidth ( $\underline{BW}$ ) of the ship's motion process transfer function  $\underline{G}_s(\omega)$  is obtained:

$$\underline{BW} = \omega_0 \left[ \sqrt{1 + 2\xi} - \sqrt{1 - 2\xi} \right] \text{ rad sec}^{-1} \text{ centered at } \omega_0 \quad (2)$$

For  $\omega_0 = 0.6 \text{ rad sec}^{-1}$  and  $\xi = 0.05$ ,  $\underline{BW} \cong 0.1 \omega_0 = 0.06 \text{ rad sec}^{-1}$ . Idealized narrow-band random processes, also called ideal bandpass stochastic processes, have been studied by Rice [10], who obtained valuable theoretical results. In particular, the autocorrelation formula and the probability distribution of zero crossing for the ideal bandpass process are given. In this paper we will validate those results, comparing them for our particular problem of ship motion predictability.

Once  $\underline{G}_s(s)$  is obtained, it is necessary to express it equivalently in the state space form. The equations take the form of a pair of linear differential equations driven by a Gaussian white noise process. The  $\underline{s}$  in the numerator of (1) normally implies that the derivative of the input function  $\underline{u}(t)$  is to be used as a forcing term in the state space representation. To avoid differentiating the random process, an adequate transformation was performed [11] with the following set of differential equations being obtained, where  $\underline{x}(t)$  represents either pitch or heave,  $\underline{u}(t)$  is the scalar random input,  $\underline{v}(t)$  is scalar noise in the measurements, and the dot indicates the time derivative:

$$\dot{\underline{x}} = \underline{A}\underline{x} + \underline{b}\underline{u} \quad (3a)$$

$$\underline{y} = \underline{c}^T \underline{x} + \underline{v}. \quad (3b)$$

In (3), the following is obtained from (1):

$$\underline{A} = \begin{bmatrix} 0 & 1 \\ -\underline{d} & -\underline{a} \end{bmatrix} \quad (4a)$$

$$\underline{b}^T = [\underline{g}, -\underline{g}\underline{a}] \quad (4b)$$

$$\underline{c}^T = [1, 0]. \quad (4c)$$

The following assumptions are made with respect to the noise and the input:

$$\underline{E} [\underline{u}] = \underline{E} [\underline{v}] = \underline{E} [\underline{v} \ \underline{x}_1] = 0 \quad (5a)$$

$$\underline{E} [\underline{u}(t) \ \underline{u}(s)] = \underline{Q} \cdot \delta(t-s) \quad (5b)$$

$$\underline{E} [\underline{v}(t) \ \underline{v}(s)] = \underline{R} \cdot \delta(t-s). \quad (5c)$$

The system of equations (3) is controllable and observable. In these equations,  $\underline{x}_1(\underline{t})$  in  $\underline{x}^T = (\underline{x}_1, \underline{x}_2)$  represents position, either heave or pitch angle. Equations (5a) through (5c) express the assumption that the ship motion and the measurement noise are uncorrelated.

### III. The Predictor Equations

Several approaches and algorithms are available for obtaining  $\underline{x}(\underline{t}+\tau)$ , the prediction of  $\underline{x}(\underline{t})$  at  $\tau > 0$  seconds from now:

- 1) the Wiener approach [12], [13], which assumes stationarity, a plausible assumption over the short periods of time required for landing;
- 2) the Ragazzini-Zadeh approach [13], [14], which is useful for the finite-time measurement case, but is otherwise complex;
- 3) the time series analysis and prediction algorithm [15];
- 4) the Kalman predictor approach [16], [17].

The last approach is adopted here because, in avoiding cumbersome computations, it makes real-time digital computation possible.

The best estimate of the ship's motion at time  $\underline{t}$ ,  $\underline{t} \in [0, \underline{t}_f]$  is denoted by  $\hat{\underline{x}}(\underline{t})$ . It is the conditional expectation of  $\underline{x}(\underline{t})$  based on all prior measurements  $\underline{y}(\underline{t})$ . Then the linear least-squares prediction theory of Kalman [16], [17] gives for the best predicted motion,  $\hat{\underline{x}}(\underline{t}+\tau)$ , the expression:

$$\hat{\underline{x}}(\underline{t}+\tau) = \phi(\underline{t}+\tau, \underline{t}) \hat{\underline{x}}(\underline{t}) \quad (6)$$

where  $\phi(\underline{t}, \sigma)$  is the transition matrix for (3).

The computation process for  $\hat{\underline{x}}(\underline{t} + \tau)$ , therefore, divides into the following two steps: 1) calculate  $\hat{\underline{x}}(\underline{t})$ ; then 2) use (6) to obtain  $\hat{\underline{x}}(\underline{t} + \tau)$  for the desired prediction  $\tau$  (see Fig. 3).

Fig 3

Since the Kalman formulation was adopted to enable real-time digital computation, (3) - (6) should be replaced by their discrete form. The discrete-time representation of the ship motion is given by:

$$\underline{x}_k = \phi_{k,k-1} \underline{x}_{k-1} + \Gamma_{k-1} \underline{u}_{k-1} \quad (7a)$$

$$\underline{y}_k = \underline{c}^T \underline{x}_k + \underline{v}_k \quad (7b)$$

where:

$$\phi_{k,k-1} = \begin{bmatrix} 1 & T_s \\ -dT_s & 1-aT_s \end{bmatrix}, \quad \Gamma_{k-1} = \begin{bmatrix} gT_s \\ -agT_s \end{bmatrix}$$

$\underline{v}_k$  = a sequence of random uncorrelated measurement noise:  $E(v_k v_j) = R_k \delta_{kj}$

$\underline{u}_k$  = a sequence of random uncorrelated inputs:  $E(u_k u_j) = Q_k \delta_{kj}$

$T_s$  = the sampling time.

The discrete-time version of the optimum filter is obtained from the following set of equations:

$$\hat{\underline{x}}_k = \phi_{k,k-1} \hat{\underline{x}}_{k-1} + K_k [y_k - \underline{c}^T \phi_{k,k-1} \hat{\underline{x}}_{k-1}] \quad (8a)$$

$$K_k = P_k' \underline{c}^T [C_k P_k' C_k^T + R_k]^{-1} \quad (8b)$$

Note that the measurement vector "c" has been replaced for convenience by a matrix "C" where:  $C_k \triangleq \begin{bmatrix} 1 & 0 \\ 0 & 0 \end{bmatrix}$ .

The a posteriori covariance matrix is obtained from:

$$P_k' = \phi_{k,k-1} P_{k-1} \phi_{k,k-1}^T + Q_{k-1} \quad (8c)$$

and the a priori covariance matrix is given by:

$$\underline{P}_{-k} = \underline{P}_{-k}^{\prime} - \underline{K}_{-k} \underline{C} \underline{P}_{-k}^{\prime} \quad (8d)$$

$\underline{P}_{-k}^{\prime}$ ,  $\underline{P}_{-k}$ , and  $\underline{K}_{-k}$  (the Kalman filter gain) are square matrices. By time  $k$ , as a result of (8a) through (8d), the best estimate  $\hat{\underline{x}}_k$ :  
 $[\hat{\underline{x}}_k \mid$  "past" values of  $\underline{y}_k$ ],  $\forall k \in [0, N]$  is generated.

The initial value of the error covariance matrix  $\underline{P}_{-k}$  is given by the matrix:

$$\underline{P}_{-0} = \overline{\underline{x}_0 \underline{x}_0^T} \quad (8e)$$

which is used as a startup value for the recursive scheme.

In this specific case we have to compute only two optimal gains, namely  $\underline{K}_{11k}$  and  $\underline{K}_{21k}$ , given by:

$$\underline{K}_{11k} = \underline{P}_{11k}^{\prime} / (\underline{P}_{11k}^{\prime} + \underline{R}_{11k}) \quad ; \quad \underline{K}_{21k} = \underline{P}_{21k}^{\prime} / (\underline{P}_{11k}^{\prime} + \underline{R}_{11k}) \quad (9)$$

The predicted vector  $\hat{\underline{x}}(\underline{t}+\tau)$  is obtained from (10) which is the discrete equivalent of (6):

$$\hat{\underline{x}}_{-k+m} = \phi(k+m, k) \hat{\underline{x}}_k \quad (10)$$

where  $\underline{m} \stackrel{\Delta}{=} \tau / T_s$ .

The transfer matrix  $\phi(k+m, k)$  is given by:

$$\phi(k+m, k) \stackrel{\Delta}{=} \phi(\tau) = e^{(-a/2)\tau}$$

$$\begin{bmatrix} \cos \beta\tau + (a/2\beta) \sin \beta\tau & (1/\beta) \sin \beta\tau \\ (-d/\beta) \sin \beta\tau & \cos \beta\tau - (a/2\beta) \sin \beta\tau \end{bmatrix} \quad (11)$$

and  $\beta^2 \stackrel{\Delta}{=} d - a^2/4$ .

Finally, since we are interested only in  $\hat{x}_1(\underline{t}+\tau)$ , the ship's optimal predicted value for  $\tau$  seconds ahead, one obtains the following result:

$$\hat{x}_1(\underline{t}+\tau) = e^{(-\underline{a}/2)\tau} [(\cos \beta\tau + (\underline{a}/2\beta) \sin \beta\tau) \hat{x}_1(\underline{t}) + (1/\beta) \sin \beta\tau \cdot \hat{x}_2(\underline{t})]. \quad (12)$$

For a narrow-band process, which is the present case, the parameter  $\underline{a}$  in (12) is very small. Thus, for moderate prediction times, (12) can be approximated by:

$$\hat{x}_1(\underline{t}+\tau) \approx \hat{x}_1(\underline{t}) \cos \beta\tau + \hat{x}_2(\underline{t}) (\sin \beta\tau)/\beta. \quad (15)$$

Equation (13), which will be used later in calculating the auto-correlation function, shows that under the stated conditions, the extrapolation is equivalent to predicting the state of an harmonic oscillator on the basis of an estimate of its present state. That this approximation is appropriate is easy to see from the quality of the prediction, results of which will be discussed next.

#### IV. Results and Discussion

Fig 4 & 5

The data shown in Figs. 4 and 5 summarize the results of a large number of cases investigated by a digital simulation of the ship's motion and its prediction. The figures show the effect of the prediction time  $\tau$  in terms of two performance criteria of significance in the carrier landing problem.

The first,  $J_1$ , measures performance in terms of the error in

predicting position. The error in prediction,  $\epsilon_p$ , is defined as:

$$\epsilon_p(t' + \tau) \triangleq x_1(t' + \tau) - \hat{x}_1(t' + \tau), \quad \forall t' \in [0, \underline{t}]$$

or

$$\epsilon_p(kT_s + \tau) \triangleq x_1(kT_s + \tau) - \hat{x}_1(kT_s + \tau), \quad \forall k \in [0, N]. \quad (14)$$

The criterion  $J_1$  is defined as the following scalar functional:

$$J_1 \triangleq (\sigma_{x_1})^{-1} \sqrt{(1/N+1) \sum_{k=0}^N \epsilon_p^2(kT_s + \tau)}. \quad (15)$$

The scalar  $J_1$  depends on the spectral width  $\underline{a}$  and the measurement noise covariance  $\underline{R}$ , in addition to the prediction time  $\tau$ , as Fig. 4 shows.

There it can be seen that if the measurement noise is not prohibitive, prediction times as long as 10 to 15 seconds are attainable with

reasonable accuracy. For example, a 5% measurement noise ( $\underline{R} = 0.02\sigma_{x_1}^2$ ), with  $\sigma_{x_1} = 1$  meter (3.1 feet) and  $\tau = 10$  seconds, gives

$\sigma_{pr} = \sigma_{x_1} J_1 \cong 0.24$  meters (0.8 feet), which can be considered acceptable.

The results obtained during the study suggested the introduction of a second criterion with respect to the predictor quality. It covers another important practical use for the predictor, the prediction of crossover times. This second criterion is defined as follows:

$$J_2 \triangleq (\omega_0/2\pi) \sum_{i=1}^M \left| \Delta T_{\text{-CRO}}(t_i) \right| \quad (16)$$

where  $\underline{M}$  is the number of crossover points counted in the fixed, finite interval of an experiment, and

$$\Delta T_{\text{-CRO}}(\underline{t}_i) \triangleq [T_i : x(t_i + \tau) = 0] - [T_i : \hat{x}(t_i + \Delta t_i + \tau) = 0] \quad (17)$$

where

$$0 \leq \Delta t_i < t_{i+1} - t_i$$

Here  $T_i : x(t_i + \tau)$  means the  $i$ th time that  $x$  crosses zero. Thus  $\Delta T_{\text{-CRO}}$  is defined as the difference between the crossover time of  $x_1(t + \tau)$  and the nearest successive crossover time of  $\hat{x}_1(t + \tau)$ . It tells how long the actual ship heave, for example, differs in sign from that predicted. Fig. 5 shows that this error is small, even for prediction times of 10 to 15 seconds. For example, under the same conditions just given, namely a 5% noise-to-signal ratio and a 10-second prediction time, and for  $T_0 = 2\pi/\omega_0 = 10$  seconds, the total time that the predicted motion differs in sign from the actual motion is 0.5 seconds over a measurement interval of 60 seconds. The practical implication of the results shown in Figs. 4 and 5 is clear and important: both the motion of aircraft carriers at sea and the crossover times of their motion can be predicted accurately over periods of time that are long enough to be operationally useful.

These results are in good agreement with Rice's analysis [10] of ideal narrow bandpass processes. However, the comparison has to be made with care since in our study the noise enters into the measurements as well as at the input. Furthermore, our results are derived from simulations of finite duration. Nevertheless, the fact that our results are consistent with his analysis of narrow-band noise strengthens our confidence in the predictability of the motion.



Evidence that the predictability of the motion of the carrier is due to its effective narrow-band character is seen from comparing the high correlation of our results with that to be expected of a narrow-band process. From eqn. 3.2-5 in [10] one gets the following expression for the autocorrelation function  $R(\tau)$  of such a process:

$$\underline{R}(\tau) = \sigma^2 [\sin(\pi \underline{BW} \tau) / (\pi \underline{BW} \tau)] \cos \omega_0 \tau \quad (18)$$

Setting  $\tau$  equal to an integral number of periods,  $\tau = \zeta T_0$ , where  $f_0 = 1/T_0$  is the center frequency of the bandpass (or the peak frequency of the power spectrum of the carrier's motion), one obtains:

$$\underline{R}(\tau)/\sigma^2 = \underline{R}(\zeta T_0)/\sigma^2 = \sin 0.2 \pi \zeta / 0.2 \pi \zeta. \quad (19)$$

This gives  $R(T_0) = 0.935\sigma^2$ , and  $R(2T_0) = 0.757\sigma^2$ .

These results compare well with ours; the correlation between the predicted values of  $\underline{x}_1(t)$ , namely  $\hat{\underline{x}}_1(t+\tau)$ , and their actual values is very nearly unity over times of the order of 10 to 15 seconds.

Furthermore, the influence of the process narrowness  $\underline{BW}$  can also be obtained from (18) and compared with the results in Fig. 4. The autocorrelation function  $\underline{R}(\tau)$  is a sinc function (see 18) of the bandwidth, a result which is in agreement with the results obtained in our study.

Rice also made an analysis of the expected zero crossings for a narrow-band process, and again, interpreting his formulas in our terms gives values consonant with the results shown in Fig. 5.

Eqn. 3.3-12 of reference [10] gives the expected number of zero crossings of  $\underline{x}_1(t)$  per second, as:

$$\underline{N}_z = 2 [ 1/3 (\underline{f}_h^3 - \underline{f}_l^3) / (\underline{f}_h - \underline{f}_l) ]^{1/2} \quad (20)$$

where  $f_h$  and  $f_l$  are the upper and lower frequency limits for the ideal, band limited process, and  $BW = f_h - f_l$ . When  $f_h$  approaches  $f_l$ , as in the narrow-band case,

$$N_z \approx \frac{f_h}{f_0} + \frac{f_l}{f_0} \approx 2 \frac{f_0}{f_0} \quad (21)$$

which is the number of zero crossings for a sinusoidal heave (or pitch) motion with frequency  $f_0 = \omega / 2\pi$ . This result agrees with ours (Fig. 5), even for prediction times as large as twice the period  $T_0$ .

Also from [10], the probability that a second zero crossing of  $x_1(t)$  lies within  $t$  and  $t + \Delta t$ , at a particular time  $t$ , say  $t = k\theta = k(T_0/2)$ , is given (approximately) by (22) for the ideal narrow-band process:

$$\text{pr}(n_{z_{\Delta t}}) = (1/2) (\gamma / [1 + \gamma^2 (t - k\theta)^2]^{3/2}) \quad \left| \begin{array}{l} t = k(T_0/2) + \Delta t \\ k = 1, 2, \dots \end{array} \right. \quad (22)$$

where

$$\gamma \triangleq \sqrt{3} [(f_h + f_l)^2 / BW] \quad ; \quad \theta \triangleq 1 / (f_h + f_l).$$

Equation (22) shows that the probability density is a symmetrical and decreasing function around  $t = k(T_0/2)$ , its peak value and dispersion depending on the bandwidth  $BW$ . For example, in the specific case of the ship's motion prediction, with  $BW = 0.1 f_0$  and  $T_0 = 10.45$  seconds,  $\text{pr}(n_{z_0}) = 3.46$ , whereas  $\text{pr}(n_{z_1}) \approx 0.01$ . This means that the probability of a zero crossing at  $(T_0 + 1.0 \text{ second})$  is very small (0.01). Here again, our results show a nice regularity of the

zero-crossing points which are (almost) identifiable with the zero-crossing points of an harmonic ship's motion with frequency  $f_0$ . This is, basically, the reason why it is possible to obtain a good prediction of the zero-crossing events for  $x_1(t+\tau)$ , even for relatively high values of  $\tau$ .

#### V. Conclusions

The feasibility of predicting aircraft carrier motion at sea by measuring the actual ship's position was investigated. The ship's motion mathematical model based on statistical data, such as power density spectrum representation, was established. Subsequently, a discrete-time Kalman filter-predictor adapted for real-time computation on a digital computer, was investigated. The results obtained show that a maximum achievable prediction time of up to 15 seconds can be reached within reasonable acceptable errors.

Being able to predict accurately the ship's motion can lead to an improvement of aircraft landing accuracy. This can be accomplished, for instance, by generating new terminal guidance (landing) laws making use of the future ship's position. Moreover, the possibility of prediction can eventually improve the LSO information and policy for landing acceptance or wave-off. The possibility of processing the measured motion by Fast Fourier Transform Algorithms (FFT), in order to obtain the power density spectrum for the ship's motion in real time, may lead toward an adaptive predictor scheme.

### Acknowledgment

The authors would like to thank Dr. G.A. Smith for his collaboration and stimulating discussions, and Mr. M. Nordstrom for aid in computational work.

### References

- [1] T.S. Durand, "Theory and simulation of piloted longitudinal control in carrier approach," Systems Technology Inc. Tech. Rept. 130-1, 1965.
- [2] T.S. Durand and R.J. Wasicko, "An analysis of carrier landing," AIAA Paper No. 65-791, 1965.
- [3] P. Kaplan, "A study of prediction techniques for aircraft carrier motion at sea," J. Hydronautics, vol. 3, no. 3, pp. 121-131, 1969.
- [4] R.F. Siewert and R.C. A-Harrah, "Study of terminal flight path control in carrier landings," North American Aviation Rept. NA66H-289, 1967.
- [5] J.L. Loeb, "Automatic landing systems are here," Proc. AGARD Conf. 1970, paper No. 14.
- [6] F.D. Powell and T. Theoclitus, "Study of an automatic carrier landing environment with the AN/SPN-10 Landing Control Central," Bell Aerosystems Co., Rept. 6026, 1965.
- [7] W.A. Johnson, "Analysis of aircraft carrier motions in a high sea state," Systems Technology Inc. Tech. Rept. 137-3, 1969.
- [8] AN/SPN-42 Automatic Carrier Landing System, Bell Aerospace Co. publication.

- [9] T. Kailath, "An innovations approach to least-squares estimations, Part I: Linear filtering in additive white-noise," IEEE Trans. Automatic Control, vol. AC-13, no. 6, pp. 646-655. Dec. 1968.
- [10] S.O. Rice, "Mathematical analysis of random noise," in Selected Papers on Noise and Stochastic Processes, N. Wax, Ed., Dover Publications, Inc., New York, N.Y., 1954.
- [11] K. Ogata, State Space Analysis of Control Systems. New York: Prentice Hall, 1968.
- [12] N. Wiener, Extrapolation, Interpolation and Smoothing of Stationary Time Series. New York: Wiley, 1949.
- [13] J.H. Lanning and R.H. Battin, Random Processes in Automatic Control. New York: McGraw-Hill, 1961.
- [14] J.R. Ragazzini and L.A. Zadeh, "An extension of Wiener's theory of prediction," J. Appl. Physics, vol. 21, pp. 645-655, 1950.
- [15] D.M. Jenkins and G. Box, Time Series Analysis, Forecasting and Control. San Francisco: Holden-Day, 1970.
- [16] R.E. Kalman and R.S. Bucy, "New results in linear filtering and prediction theory," Trans. ASME of Basic Engineering, vol. 831, pp. 95-108, 1961.
- [17] H.W. Sorenson, "Kalman filtering techniques," ch. 5 in Advances in Control Systems, vol. 3, pp. 219-292, 1966.

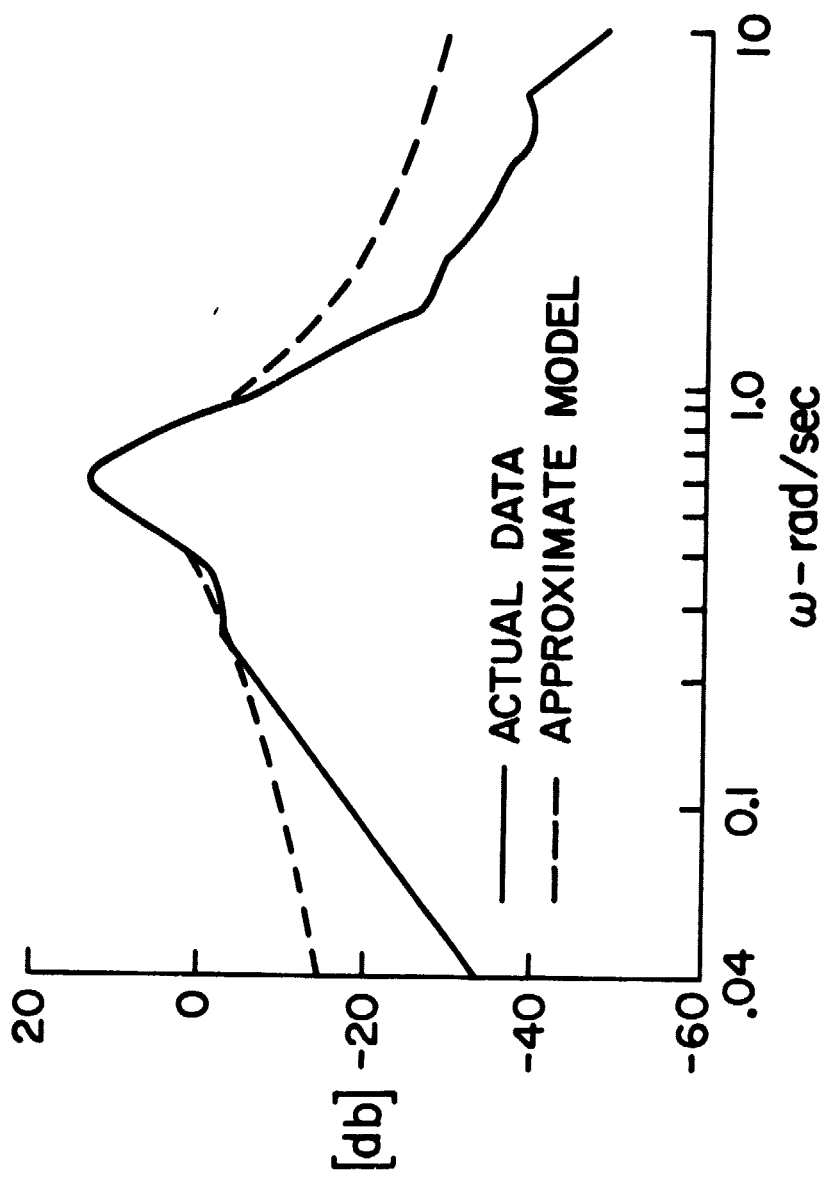
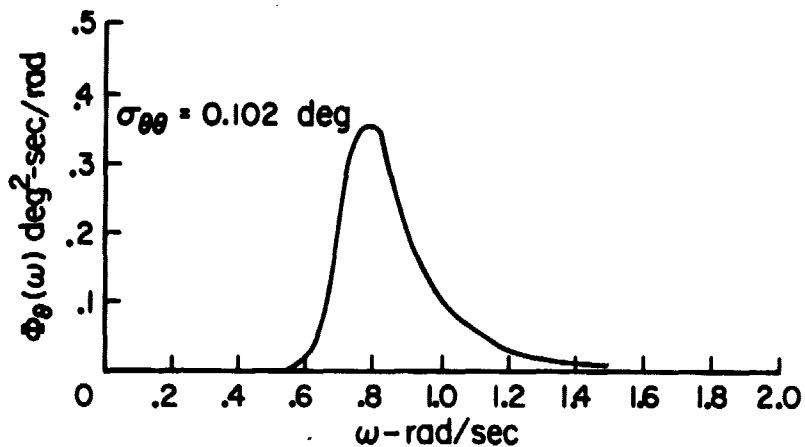


Fig. 1. Ship motion heave spectrum.

PRECEDING PAGE BLANK NOT FILMED

(a) PITCH REPRESENTATIVE POWER SPECTRAL DENSITY



(b) HEAVE REPRESENTATIVE POWER SPECTRAL DENSITY

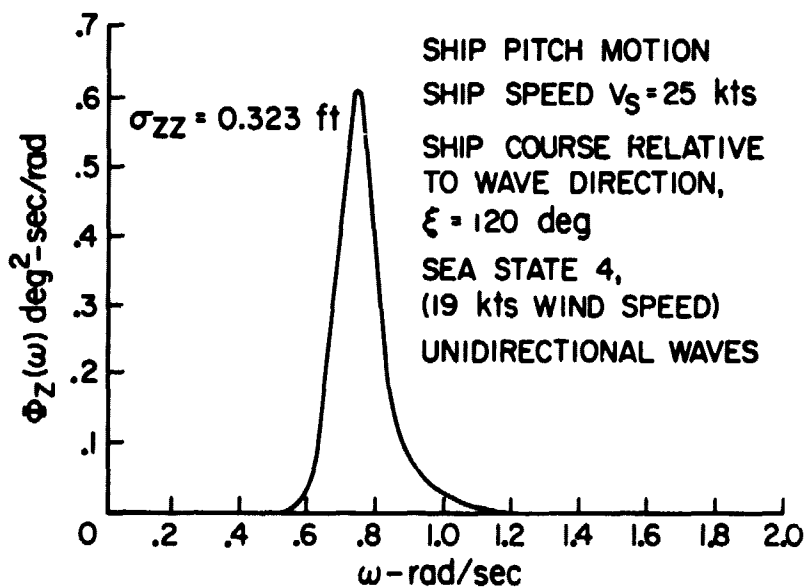


Fig. 2. Pitch and heave representative spectrum.

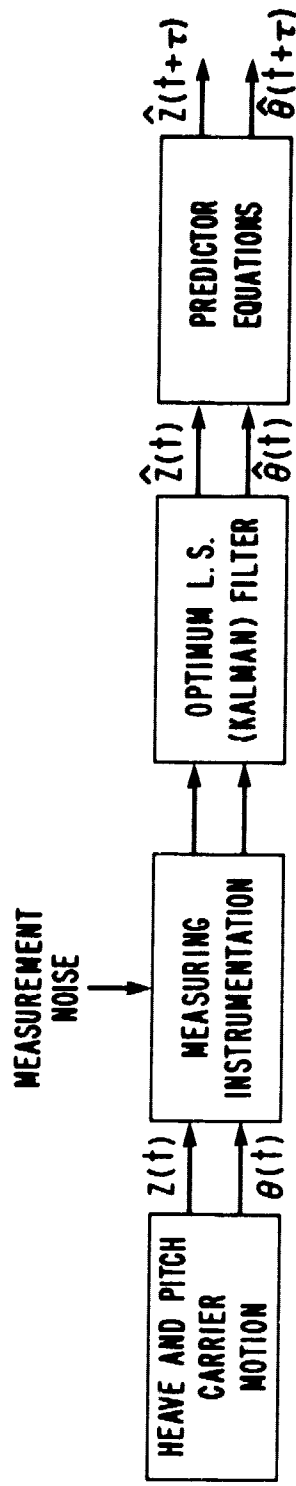


FIG. 3. Ship's motion predictor block diagram.



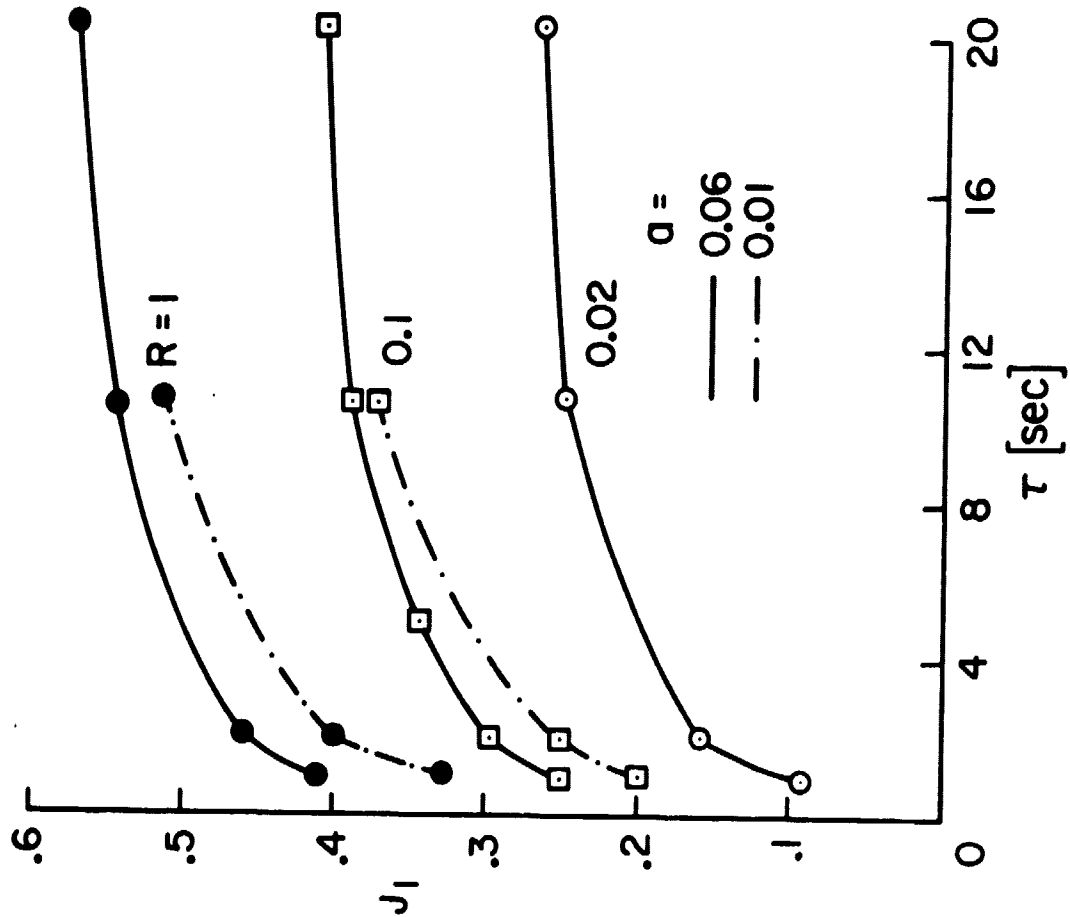


Fig. 4. Value of  $J_1$  vs. prediction time  $\tau$ .

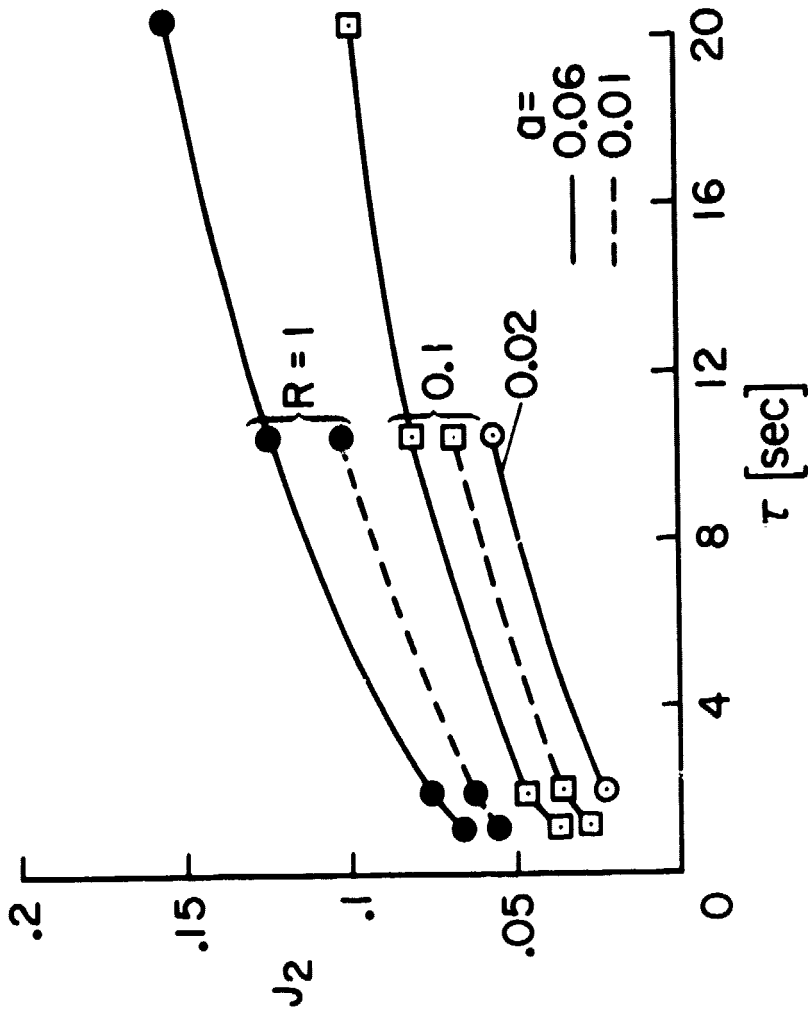


Fig. 5. Value of  $J_2$  vs. prediction time  $\tau$ .